Magnetovolume effect, macroscopic hysteresis, and moment collapse in the paramagnetic state of cubic MnGe under pressure

N. Martin,[1] M. Deutsch,[2,3] J.-P. Itié,[2] J.-P. Rueff,[2,4] U. K. Rössler,[5] K. Koepernik,[5] L. N. Fomicheva,[6] A. V. Tsvyashchenko,[6,7] and I. Mirebeau[1,*]

[1]*Laboratoire Léon Brillouin, CEA, CNRS, Université Paris-Saclay, CEA Saclay, 91191 Gif-sur-Yvette, France*

[2]*Synchrotron SOLEIL, L'Orme des Merisiers, Saint-Aubin, 91192 Gif-sur-Yvette, France*

[3]*Université de Lorraine, CRM2, UMR UL-CNRS 7036, BP 70239, 54506 Vandoeuvre-lès-Nancy, France*

[4]*Sorbonne Universités, UPMC Université Paris 06, CNRS, Laboratoire de Chimie Physique-Matière et Rayonnement, 75005 Paris, France*

[5]*IFW Dresden, P.O. Box 270116, 01171 Dresden, Germany*

[6]*Vereshchagin Institute for High Pressure Physics, Russian Academy of Science, 142190 Troitsk, Moscow, Russia*

[7]*Skobeltsyn Institute of Nuclear Physics, MSU, Vorobevy Gory 1/2, 119991 Moscow, Russia*

(Received 26 November 2015; revised manuscript received 17 May 2016; published 6 June 2016)

Itinerant magnets generally exhibit pressure-induced transitions towards nonmagnetic states. Using synchrotron-based x-ray diffraction and emission spectroscopy, the evolution of the lattice and spin moment in the chiral magnet MnGe was investigated in the *paramagnetic* state and under pressures up to 38 GPa. The collapse of the spin moment takes place in two steps. A first-order transition with a huge hysteresis around 7 GPa transforms the system from the high-spin state at ambient pressure to a low-spin state. The coexistence of spin states and observation of history-depending irreversibility is explained as the effect of long-range elastic strains mediated by magnetovolume coupling. Only in a second transition, at about 23 GPa, does the spin moment collapse.

DOI: 10.1103/PhysRevB.93.214404

Magnetism in electronic systems is fundamentally unstable with respect to lattice compression. Spin-state instabilities cause thermodynamic anomalies under temperature or pressure changes. The most famous one is the Invar effect, yielding a paused thermal expansion around room temperature in Fe-Ni and various metallic alloys [1,2], with many industrial applications. Besides thermal expansion, several physical quantities can be affected, such as the atomic volume, bulk modulus, local magnetic moment, or magnetic transition temperature. Their anomalous variations with pressure, temperature, or magnetic field are fingerprints of the Invar effect, which is still poorly understood.

Generally, it is believed that a change in the magnetovolume coupling underlies such anomalies. As assumed in the early work of Weiss [3] a "high-spin" (HS) ferromagnetic state with large atomic volume and high magnetic moment competes with a metastable "low-spin" (LS) state of reduced volume and local magnetic moment of lower magnitude. The "zero-spin" (ZS) state is a specific LS state where atoms bear no moments. These definitions were later extended to antiferromagnetic or noncollinear magnetic orders. Thermal activation of the LS state counteracts the usual expansion of the lattice with increasing temperature. Band-theory calculations later supported the basic assumption of a discontinuous transition between almost degenerated states with different moments and specific volumes in Fe-based alloys [4]. Indeed, intermediate-spin states with reduced magnetic moments have been clearly observed in transition-metal oxides [5] or molecular complexes [6]. For the metallic Invar-like systems, however, a coherent physical picture of the fundamental mechanisms underlying the magnetovolume effects could not be achieved. Attempts to go beyond the simple single-site picture proposed by Weiss involve either *magnetic* or *elastic* interactions between different sites [7]. Moreover, the existence of intermediate-spin states and discontinuous transitions is debated [8–10], while being suggested by several experiments [11–16].

In this paper, we report the observation of a clear pressure-induced first-order transition towards an intermediate LS state (at $P_{C1} \sim 7$ GPa) and a subsequent collapse of the local moment (at $P_{C2} \sim 23$ GPa) in a MnGe chiral magnet. Both transitions are observed at room temperature, far above the magnetic ordering temperature ($T_N \simeq 170$ K). Using x-ray emission spectroscopy (XES), we are able to detect the collapse of the local Mn moment in the paramagnetic regime. By measuring the lattice constant, we observe the magnetovolume effects induced by the different volumes and compressibilities of the HS and LS state. Synchrotron-based x-ray techniques are ideally suited for this task, allowing one to reach very high pressures.

The results demonstrate a discontinuous evolution and a coexistence of two microscopic spin states in an ordered metallic compound. This remarkable Invar-like effect is explained by the realization of an open two-phase system in a coherent elastic lattice [17], highlighting the importance of long-range lattice strains in the spin transition of a chemically clean system. It establishes MnGe as the first Invar chiral magnet.

MnGe belongs to the family of cubic helimagnets, where the dominant ferromagnetism competes with spin-orbit coupling resulting in long-wavelength helical spin structures. Its $B20$ structure (space group $P2_13$) is metastable at room temperature and powder samples are obtained by a high-temperature (800–2200 K) and high-pressure (2–8 GPa) quench. MnGe displays the shortest helical pitch (∼30 Å at 1.5 K) of the family [18–20], resulting in a giant topological Hall effect. To explain it, a complex skyrmion lattice was postulated,

*Corresponding author: isabelle.mirebeau@cea.fr

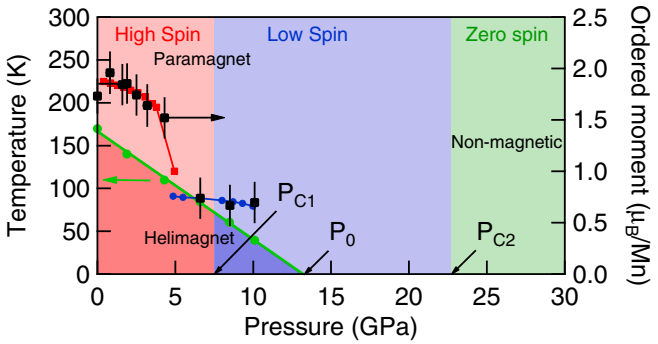

FIG. 1. (P,T) phase diagram of MnGe inferred from neutron diffraction [25] and synchrotron-based x-ray techniques (this work). The low-temperature ordered moment (black squares), ordering temperature T_N (green dots), and density function theory (DFT) calculations for HS (red dots) and LS (blue dots) states are from Ref. [25]. This work determines the critical pressures P_{C1} and P_{C2} at 300 K, from which the HS, LS, and ZS regions are drawn (red, blue, and green shaded regions, respectively).

but its existence down to T and $H \simeq 0$ is still debated [21–23]. A fluctuating inhomogeneous chiral phase takes place over a large temperature range [22]. From theory [24], the pressure-induced collapse of magnetism in MnGe should occur in two steps between HS, LS. and the nonmagnetic ZS state. High-pressure neutron diffraction [25] showed that the low-temperature ordered Mn moment decreases with increasing pressure up to a critical pressure $P_{C1} \simeq 6$ GPa, then remains constant, in excellent agreement with the calculated transition between HS and LS states. The Néel temperature T_N decreases at a rate of -14 K GPa^{-1}. At an extrapolated pressure $P_0 \simeq 13$ GPa the magnetic long-range order should vanish, but the pressure collapse between the LS and ZS state was not observed yet.

Figure 1 is the (P,T) phase diagram combining the earlier neutron data with the present x-ray results. X-ray powder diffraction (XRD) discriminates different spin states by measuring high-resolution (P,V) equations of state (EOS). XRD was performed at room temperature on the PSICHÉ beamline of the synchrotron SOLEIL, using diamond anvil cells (DAC). No indication of a structural phase transition was found up to the highest pressure of 30 GPa [26]. We therefore focus on the unit cell volume $V = a^3$, where a is the cubic lattice constant deduced from Rietveld refinements. To describe its pressure dependence, we use the *so-called* Murnaghan equation of state [27], $V(P)/V_0 = [1 + P \cdot B_0'/B_0]^{-1/B_0'}$, where B_0 is the isothermal bulk modulus, B_0' its first pressure derivative, and $V_0 = V(P \to 0)$.

In a first run, the applied pressure was increased up to ∼17 GPa—that is deeply inside the LS state—and then progressively released. The compression curve does not display a drastic change of behavior [see Fig. 2(a)]. We attribute the EOS corresponding to this process to the initial HS state which progressively transforms into the LS state. Parameters from Murnaghan EOS fit to the data are gathered in Table I. However, upon decompression, a remarkable structural hysteresis occurs, signaling the occurrence of a phase transition, across which a sizable LS proportion remains stabilized until pressure is fully released. In order to study the

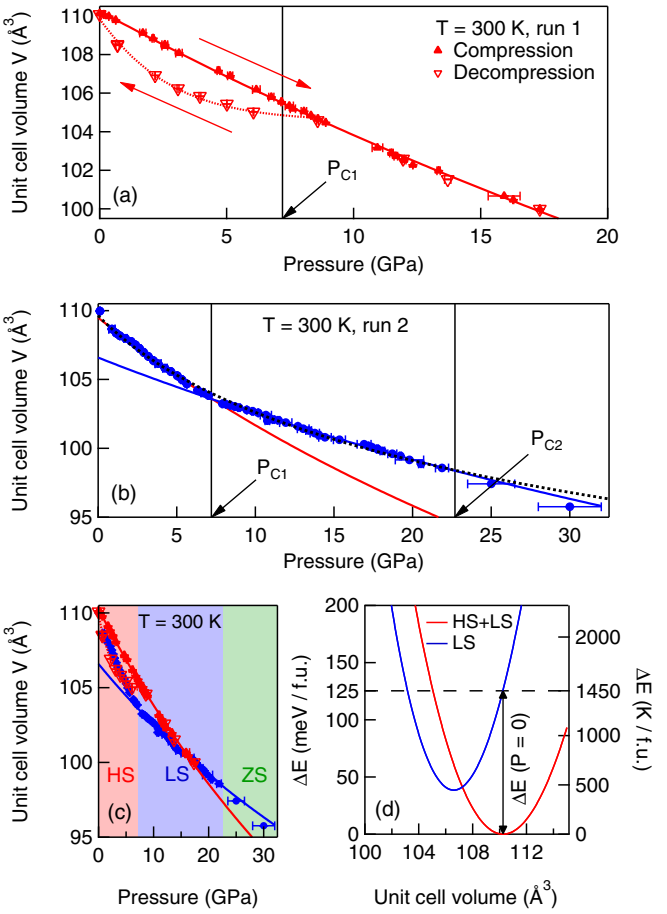

FIG. 2. Experimental (P,V) EOS of MnGe deduced from high-pressure x-ray diffraction. Results from the (a) first and (b) second run are overlayed in (c). Red and blue solid lines are Murnaghan EOS fits to the data for the low-pressure (HS+LS mixed state) and high-pressure (pure LS state) range, respectively. The dotted line in (b) is the result of a failed fit over the whole pressure range (see text). (d) Volume dependence of the energy per formula unit (f.u.) for the HS+LS and LS states of MnGe calculated from the experimental EOS.

metastability of the HS-LS microstructure, also observed in Invar alloys [28], we have prepared a second sample that was loaded in a DAC at an initial pressure of ≃7 GPa, maintained for about a week prior to the measurement. We have then quickly released the applied pressure and determined the EOS upon compression in the 0–30 GPa range. As seen on Fig. 2(b), a clear change in the EOS slope now occurs at around 7 GPa.

TABLE I. Comparison of Murnaghan EOS parameters derived from DFT and determined experimentally.

	B_0 (GPa)	B_0'	V_0 (Å^3)
HS+LS [run 1, Fig. 2(a)]	154(3)	2.6(4)	110.26(4)
HS+LS [run 2, Fig. 2(b)]	119(7)	3.4(9)	109.48(8)
LS [run 2, Fig. 2(b)]	237(3)	4.3(2)	106.6(4)
HS (DFT)	148	2.5	107.9
LS (DFT)	165	3.7	103.2
ZS (DFT)	177	4.7	102.4

A Murnaghan fit to the whole data set gives unphysical values, $B_0 = 90(5)$ GPa and a very large $B_0' = 13.5(6)$ [dotted line in Fig. 2(b)]. We conclude that the low-pressure range concerns a HS-LS composition that depends on the thermal and pressure prehistory. Considering the pressure range above 7 GPa, we obtain the parameters for the EOS in the LS state (Table I).

Our results show that a first-order transition takes place where a specific volume and compressibility are discontinuously changed. A maximal pressure of 7.2(5) GPa is estimated where the two states can coexist. Following earlier magnetic neutron diffraction results [25], we identify the coexisting two states as HS and LS states. The estimated critical pressure compares rather well with the previous determination of P_{C1}.

In Table I, density functional theory (DFT) results on the (P,V) equation of state (EOS) demonstrate the expected magnetovolume effects in the three different spin states. This calculation uses the full potential local orbital approach [29], and has an improved accuracy by using an extended set of basis states corresponding to the state of the art [30]. It yields qualitatively similar changes for the EOS between the HS and LS states as compared with experimental values (see Table I). The theoretical equilibrium volumes V_0 are lower by the fact that DFT can only reproduce the homogeneous $T = 0$ ground state (namely, it does not include thermal lattice expansion and also neglects certain effects of magnetic fluctuations). There are notable differences for the bulk moduli B_0, but our experimental and theoretical approaches agree in that the LS state possesses a smaller V_0 than the HS state, while being much less compressible. There is a remarkable history dependence of the effective EOS and hence the spin-state composition in MnGe. The difference between the compression in the first and second runs [Fig. 2(c)] proves that the internal mixed states at ambient pressure were different. The two cycles probed here, by the mixed nature of the initial states, clearly follow minor hysteresis loops.

In order to address the magnetic collapse in MnGe on a local scale, we performed hard x-ray emission spectroscopy (XES) measurements under pressure at 300 K. XES is sensitive to the local moment and earlier detected the pressure-induced collapse of magnetism in Invar alloys [14].The emission spectra were recorded up to 38 GPa on the GALAXIES beam line of the synchrotron SOLEIL (see Ref. [31]). The element-specific photon emission at the $K\beta$ line of Mn is bound to spin-sensitive selection rules. While the system is excited by the incoming photons, the final state is characterized by a core hole ($\underline{3p}$) that interacts with the $3d^n$ electrons via an intra-atomic exchange. This results in the energy splitting of the emission line (multiplet structure), yielding a main peak $K\beta_{1,3}$ at a photon energy of 6485 eV paired with a low-energy shoulder $K\beta'$ located around 6475 eV [see Fig. 3(a)].

The formal link between the spectral shape and the local moment has been well established theoretically [32,33] and the decrease in the local Mn moment upon pressure should yield a decrease in the intensity of the $K\beta'$ line relative to the main peak [34]. An absolute determination of the spin value is, however, difficult, due to the underlying multiplet structure, which does not depend only on the spin state. Moreover, in an itinerant magnet such as MnGe, the variation of the XES signal is much smaller than in more commonly studied oxides. A way to monitor the evolution of the local moment is to consider the integral $\delta(P)$ of the difference between a spectrum measured at a given pressure P with a reference spectrum (in our case measured at $P = 38$ GPa), both being normalized to unity after an appropriate background subtraction. The integral is performed around the satellite feature [gray area in Fig. 3(a)] as justified by previous works (see Ref. [35] and references therein). The method of analysis is detailed in Ref. [26]. As shown in Fig. 3, a systematic variation of the integrated difference $\delta(P)$ is observed. It decreases as pressure increases, up to about $\simeq 25$ GPa, where it saturates to 0 within error bars. This behavior reflects a second spin transition towards a state with a lower moment value than that of the LS state.

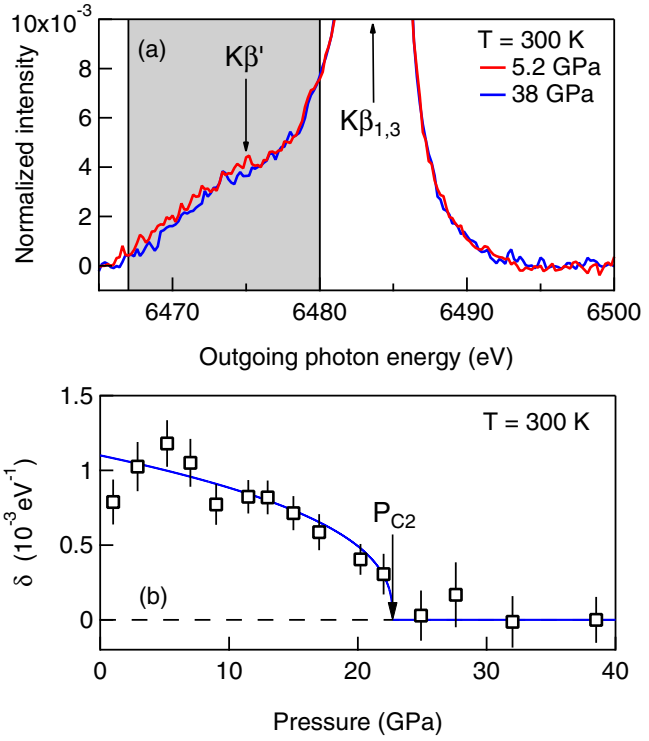

FIG. 3. (a) Typical XES response measured at room temperature at 5.2 GPa (HS+LS) and 38 GPa (ZS), illustrating the weak intensity decrease at the low-energy satellite. The gray-shaded zone denotes the energy range used for spectral integration. (b) Pressure evolution of the integrated difference $\delta(P)$ between spectra measured at each applied pressure value and the highest-pressure spectrum. The blue solid line is a power-law fit (see text).

Based on the good correspondence with DFT results [25], we identify this transition as the local LS-ZS transition expected in this pressure range as a complete collapse of spin polarization. To estimate the associated critical pressure, we have fitted the data by the power law, $\delta(P) = \delta_0(1 - P/P_{C2})^{\beta}$ for $P \leqslant P_{C2}$ and 0 otherwise, yielding a refined critical pressure $P_{C2} = 22.7(1.8)$ GPa with $\delta_0 = 1.1(1) \times 10^{-3}$ and $\beta = 0.38(15)$. Such a scaling is expected if there is a fluctuation-dominated transition from a paramagnetic to nonmagnetic state and should obey three-dimensional (3D) Ising criticality, but with pressure as the control parameter that drives the transition because of the different volumes of the LS and ZS states. On the other hand, the HS-LS transition is hardly observable using the XES technique in this metallic compound.

We also measured the evolution of the XES signal versus temperature in the range $5 \leqslant T \leqslant 300$ K at ambient pressure [26]. The data do not suggest a thermally driven HS-LS transition. Rather, a slight increase of the $K\beta'$ intensity with temperature is observed, possibly associated with a thermal repopulation in the multiplet structure. At ambient pressure the Mn local moment at 300 K is essentially in the same HS state as at low temperature in the ordered phase. This justifies *a posteriori* the x-ray experiments done at room temperature and the comparison with DFT data at 0 K, but it raises the question why the HS-LS transition does not occur with temperature as in other spin crossover compounds.

In order to answer this question, we have calculated the energy curves of the LS and ambient pressure HS state from the relation $P = -\partial E/\partial V$ by using the Murnaghan EOS [see Fig. 2(d)] with the XRD results from run 1 for the HS-LS initial mixture and run 2 for the LS state (Table I). One gets an energy gap $\Delta E \simeq 125$ meV $\simeq 1450$ K per formula unit between the two states at ambient pressure. This energy gap is larger than the temperatures where all reported magnetic measurements were performed (up to 300 K typically). It explains why no HS-LS transition occurs versus temperature. At the same time, one can also speculate that the synthesis conditions (up to 2200 K and 8 GPa) followed by a thermal quench could yield the nucleation of metastable LS states in the dominant HS state. Such a scenario would explain the large variability of magnetic properties reported in literature depending on the synthesis conditions of MnGe, which is not linked with impurities, off-stoichiometry, or random disorder.

On the other hand, the suppression of LS states in the ambient-pressure HS matrix, and their metastable coexistence implied by the pressure hysteresis, requires a coupling that prevents a simple pressure-driven transition in a jumplike process. In the paramagnetic state, where long-range magnetic order is absent, the elasticity of the lattice remains the sole explanation for the realization of two energetically different spin states in an extended pressure range. A sizable magnetovolume effect implies that the lattice is strained when locally a spin-state transition takes place. These strains effectively mediate long-range couplings between the sites that slowly decay with distance as r^{-3}, acting as an energetic barrier against a sizable nucleation of LS states [7,17,36,37]. Namely, the local strains prevent the sites from permanently occupying the minority-spin state. The spin state could be changed between HS and LS through thermal fluctuations, realizing the conditions of an "open" system. The elastic energy does not depend on the spatial arrangement of the LS sites (a fact known as the Crum-Bitter theorem for isotropic elastic two-phase bodies [36]). In the ideal case of a homogeneous system, this barrier prevents the transformation until the stability limit of the matrix phase is reached. In the real case, the coexistence of the two spin states, considered as thermodynamic phases, occurs at a microscopic level, yielding hysteresis in the physical observables. This "thermodynamics of an open two-phase system" in coherent elastic solids has been analyzed in another context by Schwarz and Khachaturyan [17,37], but it exactly applies to the case of spin-state transitions because spin states can be changed by spin-lattice relaxation [26]. Improvements to this simple thermodynamic picture may introduce certain correlations between sites of the nucleating phase, e.g., by the elastic anisotropy of the cubic lattice, but cannot fundamentally change this physical picture.

In conclusion, the magnetic collapse in MnGe occurs in two steps, in the paramagnetic regime as well as in the magnetically ordered state. The direct observation of the ultimate collapse ascertains the nature of the intermediate phase, which at low temperatures is a weak itinerant band ferromagnetic state. This somewhat contrasts with high-pressure studies in other $B20$ helimagnets such as MnSi and FeGe, where quantum phase transitions towards a nonmagnetic state have been found with intermediate regimes characterized by a non-Fermi-liquid character and/or a partial magnetic order [38,39]. The huge pressure hysteresis at the transition between the ambient paramagnetic and the pressure-induced intermediate phase proves the coexistence of different spin states. The thermodynamic anomalies, in particular, the strong irreversibility marking the pressure-induced transformation in MnGe, can be explained by the long-range strains through the magnetovolume effect. Anomalous nonequilibrium and transport behaviors are also necessarily associated with the magnetovolume effects, as observed in classical Invar alloys. Hence, the coexistence of spin states, extending down to ambient pressure at room temperature in MnGe, should influence the anomalous helimagnetic fluctuations and transport properties of MnGe.

We warmly thank F. Baudelet, L. Nataf, and P. Zerbino for experimental assistance. We acknowledge SOLEIL for provision of synchrotron radiation facilities (Proposals No. 20140163 and No. 201440217). The postdoctoral training of N.M. is funded by the LabEx Palm, through a public grant from the "Laboratoire d'Excellence PhysicsAtom Light Matter" (LabEx PALM) overseen by the French National Research Agency (ANR) as part of the "Investissements d'Avenir" program (Grant No. ANR-10-LABX-0039). L.N.F. and A.V.T. acknowledge the support of the Russian Foundation for Basic Research (Grant No. 14-02-00001).

[1] C. E. Guillaume, C. R. Acad. Sci. Paris **125**, 235 (1897).
[2] E. Wasserman, *Handbook of Ferromagnetic Materials* (Elsevier, Amsterdam, 1990), Vol. 5, pp. 237–322.
[3] R. Weiss, Proc. Phys. Soc. **82**, 281 (1963).
[4] V. L. Moruzzi, P. M. Marcus, K. Schwarz, and P. Mohn, Phys. Rev. B **34**, 1784 (1986).
[5] A. Podlesnyak, S. Streule, J. Mesot, M. Medarde, E. Pomjakushina, K. Conder, A. Tanaka, M. W. Haverkort, and D. I. Khomskii, Phys. Rev. Lett. **97**, 247208 (2006).
[6] A. Slimani, F. Varret, K. Boukheddaden, D. Garrot, H. Oubouchou, and S. Kaizaki, Phys. Rev. Lett. **110**, 087208 (2013).

[7] D. I. Khomskii and F. V. Kusmartsev, Phys. Rev. B **70**, 012413 (2004).

[8] M. van Schilfgaarde, I. Abrikosov, and B. Johansson, Nature (London) **400**, 46 (1999).

[9] P. Brown, K. Neumann, and K. Ziebeck, J. Phys.: Condens. Matter **13**, 1563 (2001).

[10] K. Matsumoto, H. Maruyama, N. Ishimatsu, N. Kawamura, M. Mizumaki, T. Irifune, and H. Sumiya, J. Phys. Soc. Jpn. **80**, 023709 (2011).

[11] M. M. Abd-Elmeguid and H. Micklitz, Phys. Rev. B **40**, 7395(R) (1989).

[12] S. Odin, F. Baudelet, C. Giorgetti, E. Dartyge, J. Itié, A. Polian, J. Chervin, S. Pizzini, A. Fontaine, and J. Kappler, Europhys. Lett. **47**, 378 (1999).

[13] L. Dubrovinsky, N. Dubrovinskaia, I. A. Abrikosov, M. Vennström, F. Westman, S. Carlson, M. van Schilfgaarde, and B. Johansson, Phys. Rev. Lett. **86**, 4851 (2001).

[14] J. P. Rueff, A. Shukla, A. Kaprolat, M. Krisch, M. Lorenzen, F. Sette, and R. Verbeni, Phys. Rev. B **63**, 132409 (2001).

[15] F. Decremps and L. Nataf, Phys. Rev. Lett. **92**, 157204 (2004).

[16] T. Yokoyama and K. Eguchi, Phys. Rev. Lett. **107**, 065901 (2011).

[17] R. B. Schwarz and A. G. Khachaturyan, Phys. Rev. Lett. **74**, 2523 (1995).

[18] N. Kanazawa, Y. Onose, T. Arima, D. Okuyama, K. Ohoyama, S. Wakimoto, K. Kakurai, S. Ishiwata, and Y. Tokura, Phys. Rev. Lett. **106**, 156603 (2011).

[19] O. L. Makarova, A. V. Tsvyashchenko, G. Andre, F. Porcher, L. N. Fomicheva, N. Rey, and I. Mirebeau, Phys. Rev. B **85**, 205205 (2012).

[20] S. V. Grigoriev, N. M. Potapova, S.-A. Siegfried, V. A. Dyadkin *et al.*, Phys. Rev. Lett. **110**, 207201 (2013).

[21] N. Nagaosa and Y. Tokura, Nat. Nanotechnol. **8**, 899 (2013).

[22] M. Deutsch, P. Bonville, A. V. Tsvyashchenko, L. N. Fomicheva, F. Porcher, F. Damay, S. Petit, and I. Mirebeau, Phys. Rev. B **90**, 144401 (2014).

[23] R. Viennois, C. Reibel, D. Ravot, R. Debord, and S. Pailhès, Europhys. Lett. **111**, 17008 (2015).

[24] U. Rössler, J. Phys.: Conf. Ser. **391**, 012104 (2012).

[25] M. Deutsch, O. L. Makarova, T. C. Hansen, M. T. Fernandez-Diaz, V. A. Sidorov, A. V. Tsvyashchenko, L. N. Fomicheva, F. Porcher, S. Petit, K. Koepernik *et al.*, Phys. Rev. B **89**, 180407 (2014).

[26] See Supplemental Material at http://link.aps.org/supplemental/10.1103/PhysRevB.93.214404 for details about experimental conditions, data analysis strategy, and further theoretical considerations.

[27] F. Murnaghan, Proc. Natl. Acad. Sci. USA **30**, 244 (1944).

[28] P. Gorria, D. Martínez-Blanco, M. J. Pérez, J. A. Blanco, A. Hernando *et al.*, Phys. Rev. B **80**, 064421 (2009).

[29] K. Koepernik and H. Eschrig, Phys. Rev. B **59**, 1743 (1999).

[30] K. Lejaeghere *et al.*, Science **351**, 6280 (2016).

[31] J.-P. Rueff, J. M. Ablett, D. Céolin, D. Prieur, T. Moreno, V. Balédent, B. Lassalle-Kaiser, J. E. Rault, M. Simon, and A. Shukla, J. Synchrotron Radiat. **22**, 175 (2015).

[32] G. Peng, F. de Groot, K. Hämäläinen, J. Moore, X. Wang, M. Grush, J. Hastings, D. Siddons, W. Armstrong, O. Mullins *et al.*, J. Am. Chem. Soc. **116**, 2914 (1994).

[33] G. Vankó, T. Neisius, G. Molnár, F. Renz, S. Kárpáti, A. Shukla, and F. de Groot, J. Phys. Chem. B **110**, 11647 (2006).

[34] A. Mattila, J.-P. Rueff, J. Badro, G. Vankó, and A. Shukla, Phys. Rev. Lett. **98**, 196404 (2007).

[35] Z. Mao, J.-F. Lin, J. Yang, J. Wu, H. C. Watson, Y. Xiao, P. Chow, and J. Zhao, Am. Mineral. **99**, 415 (2014).

[36] P. Fratzl, O. Penrose, and J. L. Lebowitz, J. Stat. Phys. **95**, 1429 (1999).

[37] R. Schwarz and A. Khachaturyan, Acta Mater. **54**, 313 (2006).

[38] C. Pfleiderer, D. Reznik, L. Pintschovius, H. v. Lohneysen, M. Garst, and A. Rosch, Nature (London) **427**, 227 (2004).

[39] A. Barla, H. Wilhelm, M. K. Forthaus, C. Strohm, R. Rüffer, M. Schmidt, K. Koepernik, U. K. Rößler, and M. M. Abd-Elmeguid, Phys. Rev. Lett. **114**, 016803 (2015).